 doi:10.20944/preprints202210.0175.v1

A CNT toughened strategy used for in-situ repair of aircraft composite structure

Tengfei Yang[1], Bin Liu[1*], Fei Xu[1], Bo Wang[1], Chengwei Wu[3**]

1. School of Aeronautics, Northwestern Polytechnical University, Xi'an, China

2. Department of Engineering Mechanics, State Key Laboratory of Structural Analysis for Industrial Equipment, Dalian University of Technology, Dalian, China

Abstract

This study aims to develop an in-situ field repair approach, special for aircraft composite structures, to enhance the interlaminar toughness of plain woven composites (PWCs) by adding multi-walled carbon nanotubes (MWCNTs). MWCNTs are dispersed at each interface between prepreg layers by means of solvent spraying with the density is 1.58 g/m^2. And then, the layers are stacked with the predefined sequence and cured at 120℃ and 1 bar pressure using the heat repairing instrument. Moreover, double cantilever beam (DCB) standard test is used to investigate the interlaminar toughening effect due to the MWCNTs. For comparison, original samples are also prepared, the results indicate that the introduction of MWCNTs can favorably enhance the interlaminar toughness of PWCs at field repair approach and the Mode I fracture energy release rate G_{IC} increases by 102.92%. Based on finite element method (FEM) of continuum damage mechanics, the original and MWCNTs toughening specimen under DCB Mode I fracture are modeled and analyzed. The simulation and experiment are in good agreement. Finally, the toughening mechanism of MWCNTs is explored by scanning electron microscope (SEM), it is founded that a large amount of Fiber-matrix (F-M) interface debonding and matrix cracking of mountain shape are the major modes of fracture accompanied with few fiber breakage and matrix peeling off for the MWCNTs toughening specimens.

Keywords: CNT; in-situ repair；Fractsure toughness；Cohesive interface modelling

Preprints (www.preprints.org) | NOT PEER-REVIEWED | Posted: 12 October 2022 doi:10.20944/preprints202210.0175.v1

1. Introduction

Carbon fiber reinforced polymer (CFRP) composites are being increasingly used in aeronautical fields due to their remarkable excellent properties, such as high strength, high modulus, light weight, good heat-resistance, good fatigue resistance, etc.
Composite materials account for an increasing proportion in the new generation of advanced aircrafts, such as B787, A350XWB, the fraction of composite materials even accounts for more than fifty percent. Even though CFRP composites have excellent in-plane properties, it is susceptible to delamination caused by low-velocity impacts (e.g. drop tools, hails, sands) due to their low interlaminar toughness. Moreover, delamination is also likely to reduce the mechanical properties of CFRP composites, especially the compressive strength after impact, which is the key indicator of impact damage tolerance[1][2]. Therefore, it is necessary to study the interlaminar fracture performance of CFRP composites, explore the ways to improve it and reveal its mechanism.

In most of the existing studies, researchers have studied interlaminar strength and fracture toughness of CFRP composites using different methods from various perspectives. Several techniques have been successfully devised to enhance the delamination resistance[3][8], namely designing 3D fabric architecture**Error! Reference source not found.**[3], transversely stitching or pinning the fabrics**Error! Reference source not found.**[6], fiber hybridization**Error! Reference source not found.**, toughening matrix material**Error! Reference source not found.**, placing interleaves between the plies**Error! Reference source not found.** etc. These technologies had been proven to improve the interlaminar fracture toughness, while sacrificing the in-plane mechanical properties or increasing the thickness of CFRP laminates. Till 1991, carbon nanotubes (CNTs)[9] founded by Lijima brought a promising opportunity to significantly enhance the interlaminar toughness without weakening the in-plane properties or enlarging the thickness. Hamer et al.[10] utilized multi-walled carbon nanotubes (MWCNTs) reinforced electrospun Nylon 66 interleaving to improve the Mode I and Mode II fracture toughnesses of CFRP laminates. The MWCNTs-reinforcement can effectively resist the crack continuously propagating between the adjacent plies. Therefore, the reinforced CFRP laminates required 400% and 160% Mode I and Mode II fracture energies, compared with the non-reinforced ones. Joshi et al.[11] proposed a novel method for dispersing MWCNTs onto the woven CFRP prepregs, and the interlaminar fracture toughnesses of CFRP laminates with different MWCNTs densities were evaluated by double cantilever bending (DCB) and end notch flexure (ENF) tests. The results showed that, the addition of MWCNTs between the CFRP prepregs helps in strengthening the interface and fracture toughnesses, and the optimal MWCNTs density was identified as 1.32 g/m^2 at the midplane, in which case G_{IC} and G_{IIC} were enhanced by 32% and 140% at crack propagation, respectively. Tong et al.[12] proposed two continuum-mechanics-based models to reveal the pull-out mechanisms of long MWCNTs by theoretical analysis and experimental observations. These two models were both employed to investigate the influence of long MWCNTs on the Mode I delamination toughness of laminated composites by numerical simulations of DCB tests. The results indicated that the addition of MWCNTs is able to improve the Mode I interlaminar fracture toughness of

Preprints (www.preprints.org) | NOT PEER-REVIEWED | Posted: 12 October 2022 doi:10.20944/preprints202210.0175.v1

the composites, and the density, length as well as the maximum pull-out displacement of MWCNTs possess significant effects on the Mode I fracture toughness.

Khan and Kim[13] fabricated bucky papers using CNTs or carbon nanofibers (CNFs), which were subsequently integrated and cured with carbon fiber prepregs to produce CFRP laminates. The shear and flexural properties of the obtained CFRP laminates were characterized by experiments. It was found that, both the interlaminar shear strength and Mode II toughness were increased by 31% and 104% for the multiscale CFRP composites, respectively. Almuhammadi et al.[14] dispersed MWCNTs on the interfaces between prepregs, the DCB experiments showed that the Mode I fracture toughness of the nano-reinforced composites was improved by 17%. Moreover, according to the scanning electron microscope (SEM) analyses of the damaged morphologies, the improvement was mainly attributed by the ability of the nano-reinforcement to prevent the damage initiation and propagation by CNTs pullout, peeling and bridging. Liu et al.[15] reported a low-cost approach by adding two different nano-materials to the interlayer surface, MWCNTs and multi-layers graphene (mG). The experimental DCB tests indicated that the values of G_{IC} are enhanced by 12.3% (MWCNTs) and 101.4% (mG) respectively, which was in good agreement of the simulation results. In summary, for the foregoing studies, researchers mostly focused on the autoclave or autoclave-like processes of enhancing interlaminar toughness of composites by adding nano-materials (CNTs, MWCNTs).

Autoclave is a special pressure vessel that can bear and regulate a certain temperature and pressure range, and autoclave molding refers to the process of using the high-temperature and compressed gas inside the autoclave to generate pressure to heat and cure the composite prepregs. So, for the autoclave process, its main characteristics lies in the corresponding mold to ensure the shape of the structure, while providing a high pressure of more than 1 bar on the surface of the composite prepregs. These features make it suitable to manufacture or to repair of the integral structure in factory. However, in wartime or other emergency moments, it is necessary to repair the damaged parts of the composite structures effectively as soon as possible. While, with respect to autoclave process, repairing is complicated and time-consuming. In addition, the damaged parts of the composite structures need to be disassembled if possible, while large non-detachable components must be placed in an autoclave with a large or super large dimension. It definitely results in increasing the three-dimensional size of autoclave, which is especially unacceptable .

On account of the repairing problems of autoclave process, we focus on the field repair process of composite structures. Unlike the autoclave process, the field repair process is low-cost and efficient, it requires no complex instrument or equipment. For different types of damages, the field repair process requires no special mold, it relies on the original composite structures, initially grinding in the damaged components and then repairing. However, the field repair process only requires 1 bar of curing pressure by a vacuum bag, which is further lower than the high pressure required by the autoclave. Although the field repair process exhibits several advantages in recovering the damaged composite structures, whether the mechanical properties of the post-repaired structures can be kept consistent with those of undamaged structures or

Preprints (www.preprints.org) | NOT PEER-REVIEWED | Posted: 12 October 2022 doi:10.20944/preprints202210.0175.v1

improved possess significant influence on the structural safety, still forming an important concern for academic and engineering researchers.

Actually, some recent investigations have developed field repair approaches, and studied the post-repaired performance. In the work of Karuppannan et al.[16], a series of field repair work was carried out according to the damage situation, including repair patch design, fabrication and implementation of the repair. This work further revealed that CFRP patch is a feasible choice for repairing damaged metal structures. Monsalve et al.[17] selected CNTs as a reinforcement in the epoxy resin to decrease the fatigue crack propagation rate in the 2024 T3 Al alloy. The results showed that a small amount of CNTs is helpful to extend the fatigue crack propagation life of Al alloy structures. The crack initiation and propagation is dramatically delayed. When the resin matrix includes 0.5vol% and 1vol% CNTs reinforcement, the fatigue life is increased by 104% and 128% respectively. Kong et al.[18] simulated the impact damage of unidirectional CFRP composite spar structures and sandwich structures. And then, they repaired the damaged structures using the external patch repair method, and compared the compressive strengths of the repaired structures with the undamaged ones. They experimentally and numerically found that the compressive strengths of the repaired spar and sandwich structures are recovered to 91.19% and 88.68% of the undamaged ones.

Due to the excellent improvement of the mechanical properties for CFRP composites by adding MWCNTs[19][15][19], this study developed a field repair approach to enhance the interlaminar toughness of plain woven composites (PWCs) by adding MWCNTs into each interface between prepreg layers. The field repair strategy and experimental work are presented in Section 2. The experimental and simulation results are discussed and analyzed in Section 3, and the conclusions are given in Section 4.

2 Materials, specimens manufacturing and experimental procedures

2.1 Materials

The fabrics contain carbon fiber T700-3K (diameter: 7 μm) provided by Toray company, and the epoxy resin is provided by Loctite company. Their material properties are listed in Table 1. The MWCNTs are manufactured by chemical vapor deposition (CVD) approach, and the purity is greater than 95wt%. The length of the MWCNTs varies from 3 μm to 12 μm, and the internal and external diameters are 3-5 nm and 8-15 nm, respectively.

Table 1 Material properties of carbon fibers and epoxy resin

Materials	Type	Elongation to break (%)	Tensile modulus (GPa)	Tensile strength (MPa)	Density (g/cm^3)
Carbon fiber	T700-3K	2.0	240	4900	1.80
Epoxy resin	EA 9390 AERO	2.5	2.88	56.5	1.15

2.2 Specimens manufacturing

In this study, MWCNTs are utilized to enhance the interlaminar toughness of PWC laminates by a low-cost and rapid field repair strategy. The MWCNTs-based field repair technological process of composite specimens is shown in

Preprints (www.preprints.org) | NOT PEER-REVIEWED | Posted: 12 October 2022 doi:10.20944/preprints202210.0175.v1

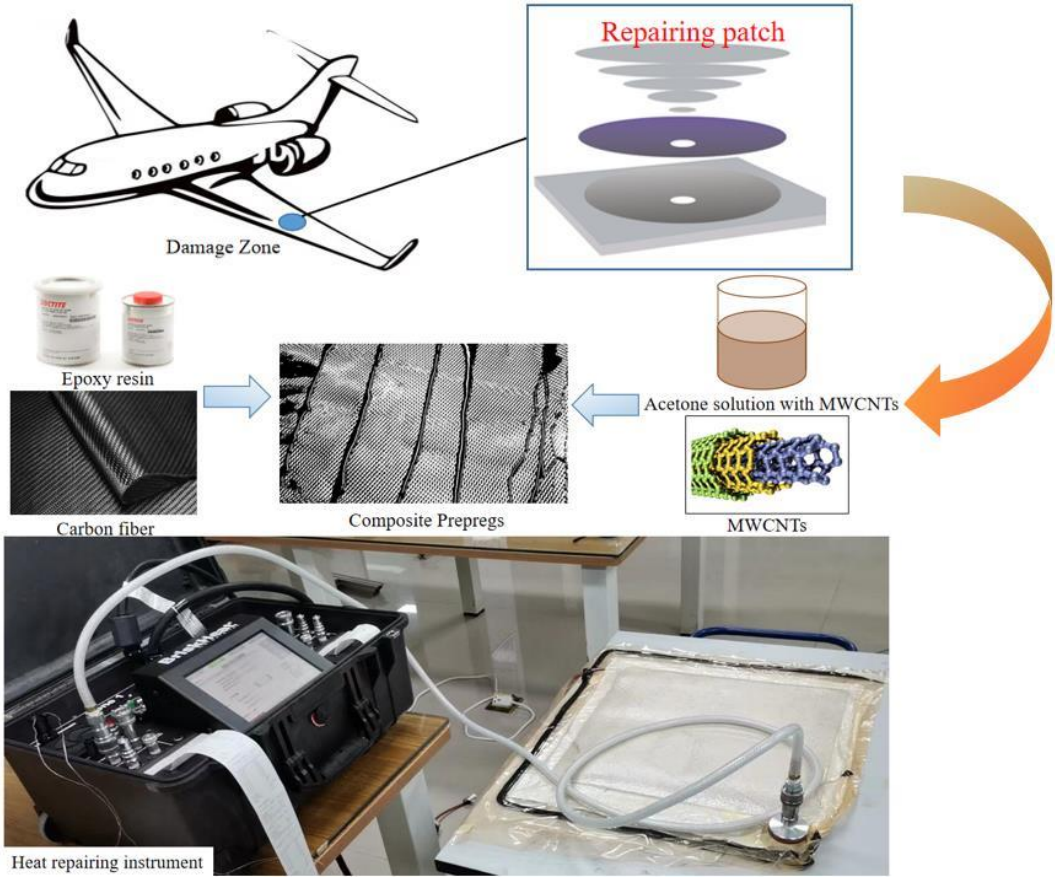

Fig. 1. The first step is to apply the epoxy resin evenly to the carbon fiber cloth to make composite prepregs. The second step is dispersing the MWCNTs into the acetone solution under ultrasonic wave for 15 mins at 23℃ (ambient temperature) to avoid the agglomeration of MWCNTs, and spraying the nano-materials solution on the each surface of prepregs. And the supplements density of 1.58 g/m^2 is chosen to investigate and obtain the interlaminar toughness enhancement. And then, 20 wet composite prepregs are totally stacked with the predefined sequence, in which the 0° and 90° plies are alternately laid. Meanwhile, polyethylene (PE) films with a thickness of 0.03 mm, are inserted between the 10-th and 11-th layers, to represent the initial Mode I cracks, namely the LVI-induced delamination. After that, the wet fabrics are cured by a heat repairing instrument with the curing temperature of 120℃ and the pressure of 1 bar for 4 h.

Preprints (www.preprints.org) | NOT PEER-REVIEWED | Posted: 12 October 2022 doi:10.20944/preprints202210.0175.v1

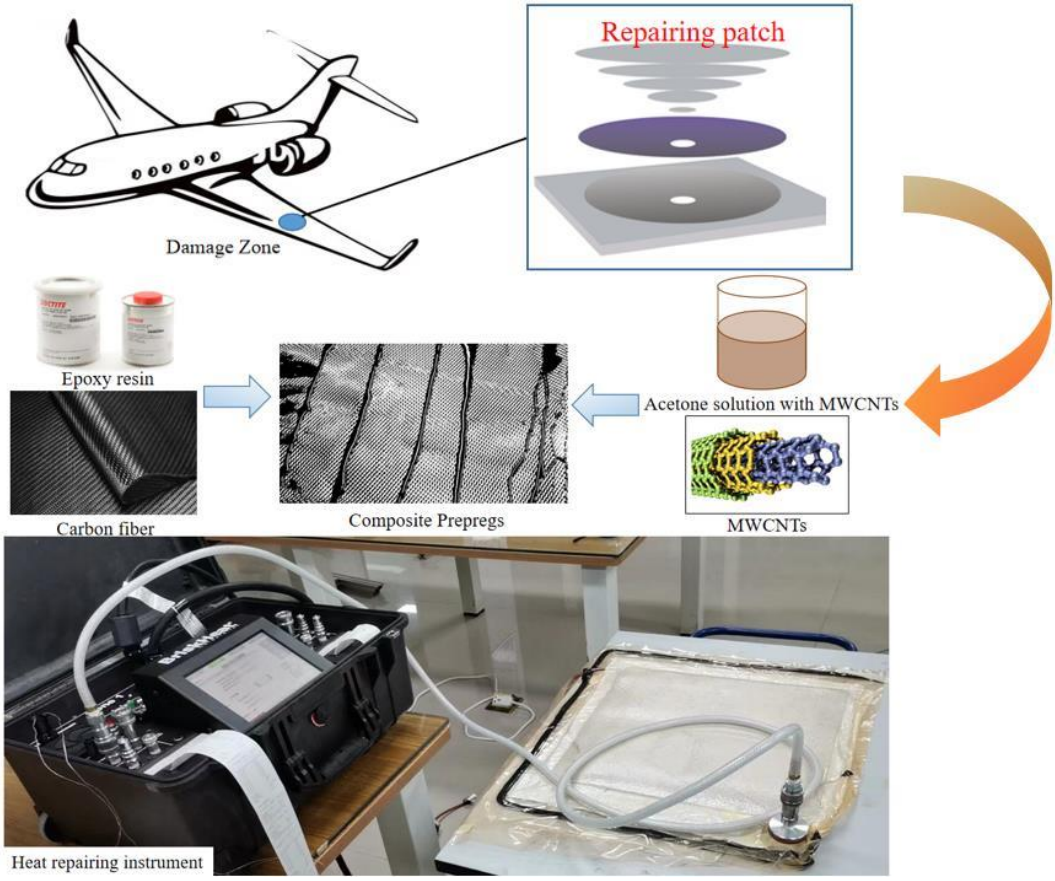

Fig. 1 Illustration of the MWCNTs-based field repair strategy

2.3 Set up and equipment

The heat repairing instrument is a comprehensive repair equipment for composite structures, capable of heating up to 760°C and vacuuming. Due to its excellent convenience and reliability, this equipment is usually used to provide curing temperature and vacuum environment for the resin curing. The heating rate, temperature maintenance time and cooling rate can be set according to the operation requirements. Besides, the heat repairing instrument possess significant advantages in repairing the composite structures with large dimension and complex shapes, because it doesn't have to disassemble the structural parts.

2.4 Double cantilever beam (DCB) set-up and tests

The CFRP laminates are obtained with a thickness of 7 mm. Besides, a group of original laminates are fabricated as the reference to evaluate the interlaminar toughening effect caused by MWCNTs. The Mode I fracture toughness tests were performed on the obtained DCB specimens according to the ASTM D5528-13 standard[20] as reference. Fig. 2 shows the schematic illustration of the DCB specimen and loading conditions. A pair of piano hinges were adhesively bonded on top and bottom sides of each DCB specimen, near to the inserted PE film. Besides, the piano hinges were fixed with the fixtures of an universal tensile testing machine. A tensile displacement perpendicular to the specimen length direction, was prescribed on the upper piano hinge to prompt the crack growth. And, a quasi-static displacement rate of 1 mm/min was used during loading process.

Preprints (www.preprints.org) | NOT PEER-REVIEWED | Posted: 12 October 2022 doi:10.20944/preprints202210.0175.v1

During the DCB testing process, the applied load and opening displacement were recorded, respectively. The onset of the delamination (namely, the Mode I crack growth) is defined by the sudden drop of the load-displacement curve. After the maximum load, the applied load nonlinearly decreases as the opening displacement continuously rises. Meanwhile, the delamination length was measured to calculate the Mode I fracture toughness. To evaluate the enhancement of interlaminar toughness, a group of original DCB specimens without adding MWCNTs were manufactured. Furthermore, each testing group included 4 specimens to ensure the reproducibility of the experimental results. Details of the experimental results are presented in Section 3.1.

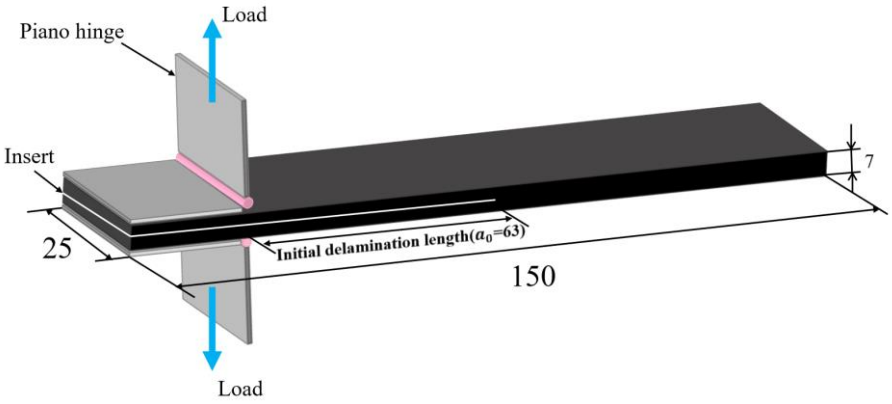

Fig. 2 Schematic illustration of the DCB specimen and loading conditions (unit: mm)

In order to eliminate the influence of the measured crack length on the fracture toughness, the total crack length a (Fig. 3) can be calculated by Eq. (1), and the Mode I energy release rate G_{IC} is calculated by Eq. (2)[21] .

$$a = \sqrt[3]{\frac{3\delta E_{11} I_Z}{2P}} \tag{1}$$

where, P is the applied load, δ is the applied displacement, E_{11} is the elastic modulus of composite materials, and I_z is the moment of inertia of one arm.

$$G_{IC} = \frac{P^2}{E_{11} I_z b} \sqrt[\frac{3}{2}]{\frac{3\delta E_{11} I_z}{2P}} \tag{2}$$

where, b is the width of the specimen.

Preprints (www.preprints.org) | NOT PEER-REVIEWED | Posted: 12 October 2022 doi:10.20944/preprints202210.0175.v1

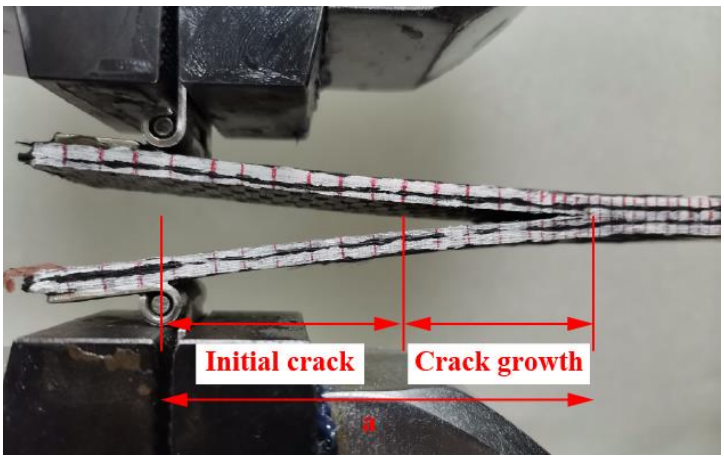

Fig. 3 Illustration of the initial crack and crack growth lengths in the DCB specimen

3. Experimental and simulation results and analysis

3.1 Experimental behavior, crack length *a* and energy release rate G_{IC}

The load-displacement curves of the Original (4 specimens) and MWCNTs toughening groups (4 specimens) are depicted in Fig. 4. As displayed in Fig. 4, the load-displacement curves possess two representative characteristics: (a) The MWCNTs toughening group has a larger opening displacement. (b) The MWCNTs toughening group possesses the larger maximum peak value of load (P_{max}) and the load drops more slowly in the descent stage, which is no sudden descent process, the overall more smooth.

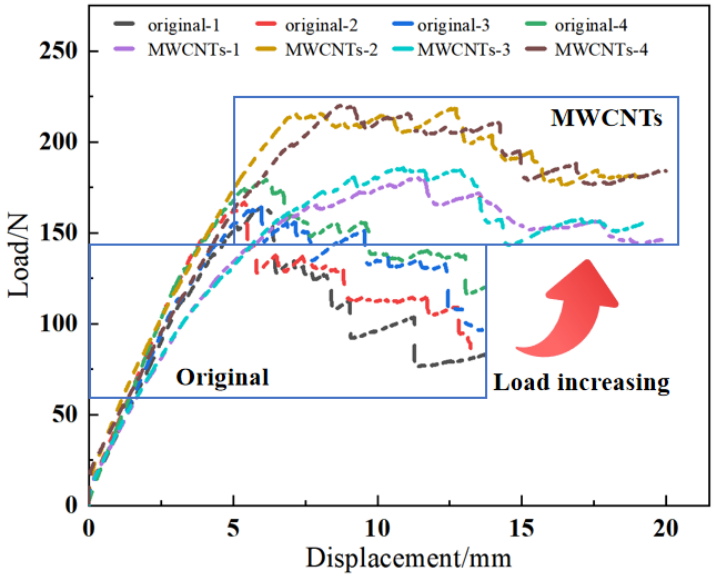

Fig. 4 Load-displacement curves from DCB Test

In order to intuitively characterize the process of DCB tests of tensile, Fig. 4 is simplified to Fig. 5, which has three obvious stages: the linear increasing stage, the nonlinear increasing stage and the nonlinear decreasing stage. As shown in Fig. 5, after the linear increasing stage and nonlinear increasing stage, the load reaches the maximum value and then enters the nonlinear decreasing stage. The maximum loads and nonlinear decreasing slopes of the original specimens and MWCNTs toughening

Preprints (www.preprints.org) | NOT PEER-REVIEWED | Posted: 12 October 2022 doi:10.20944/preprints202210.0175.v1

ones, listed in Table 2.

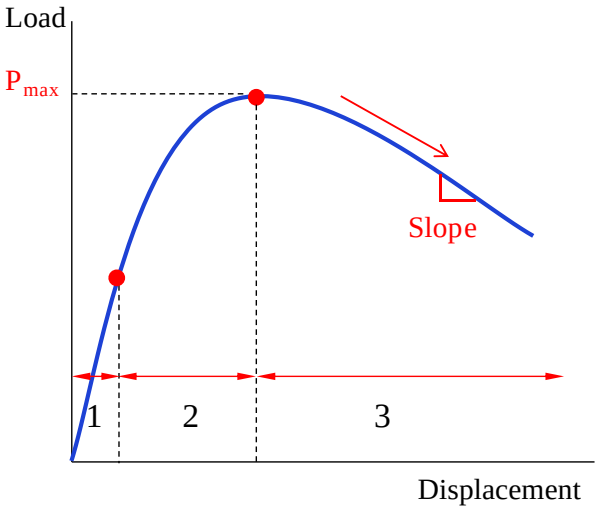

Fig. 5 The simplified load-displacement curve for DCB test

From Table 2, with regard to MWCNTs toughening specimens, the average value of P_{max} increases by 19.5%, and the slope of nonlinear decrease stage decreases by 63.8% compared with the original ones.

Table 2 The maximum loads and nonlinear decreasing slopes of the Original specimens and MWCNTs toughening ones

Specimens	P_{max}/N	Average value	Increasing rate/%	Slope/%	Average value	Decreasing rate/%
Original	163.2	168.3	-	10.9	10.5	-
	166.9			10.9		
	164.0			11.0		
	179.2			9.1		
MWCNTs toughening	180.5	201.2	19.5% ↑	3.9	3.8	63.8% ↓
	218.5			5.2		
	185.7			3.0		
	219.9			3.2		

The crack growing length a and energy release rate G_{IC} are calculated by Eq. (1) and Eq.(2) respectively, as shown in Fig. 6. The initiation value of G_{IC} have been evaluated using the load and deflection measured at the point of deviation from linearity in the load-displacement curve, which is typically the lowest among the three different G_{IC} initiation value definitions. However, this paper focuses on the comparison of the fracture toughness between the original and MWCNTs toughening specimens, so the influence could be ignored. The crack propagation can be divided into two stages: crack initiation non-stable stage (the blue color rectangular box in Fig. 6) and crack propagation stable stage (the red color rectangular box in Fig. 6). It is reasonable to choose the data from the stable crack propagation stage as G_{IC} data source as shown in Fig. 6.

Preprints (www.preprints.org) | NOT PEER-REVIEWED | Posted: 12 October 2022 doi:10.20944/preprints202210.0175.v1

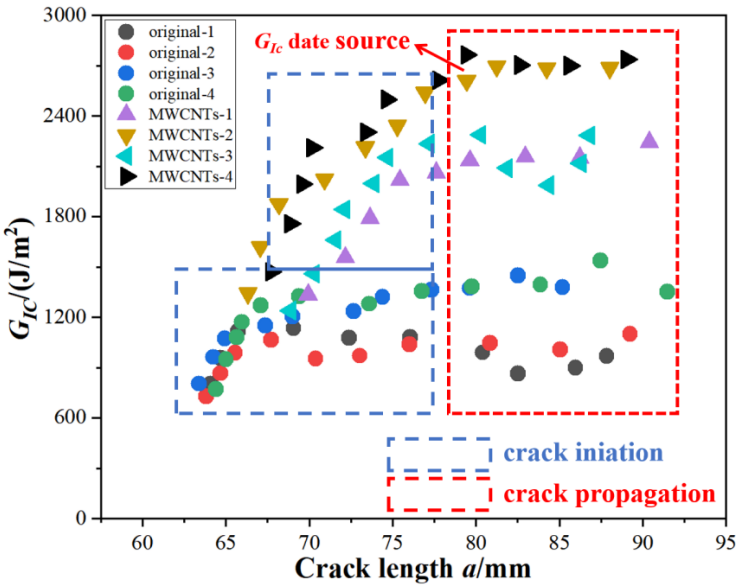

Fig. 6 The G_{IC}-a relational graph

The calculated results, as shown in Fig. 7, show that the critical energy release rate G_{IC} of MWCNTs toughening specimens in stable crack propagation stage obtains improvement of 102.92%, from 1199.15 J/m^2 (Original) to 2435 J/m^2 (MWCNTs toughening). Even though removing a group of highest value (MWCNTs-4), it still posseses 95% improvement. The imperfect aspect is the data of MWCNTs toughening is highly dispersed than original ones. According to the above analysis, the interlaminar Mode I toughness of CFRPs can be enhanced obviously by embedding MWCNTs between the adjacent laminas with the heat repairing instrument in the field repair condition.

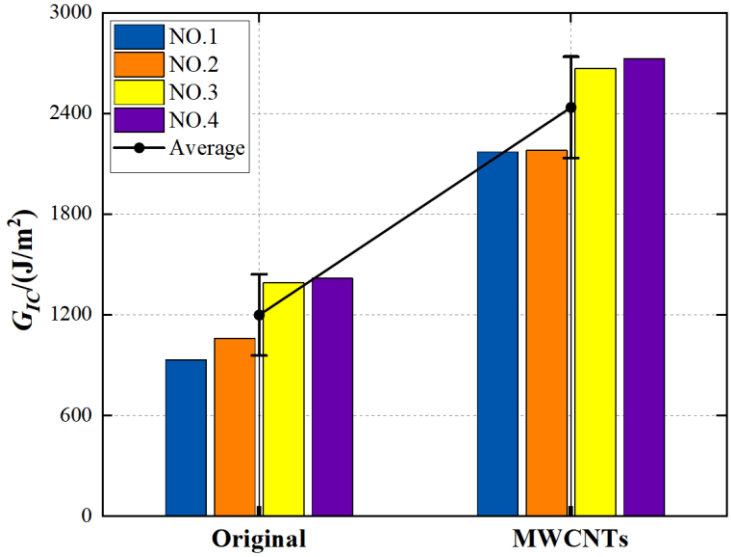

Fig. 7 The G_{IC} variation for Original and MWCNTs toughening groups

3.2 Simulation Method and Results

3.2.1 Cohesive damage theory

The bulit-in cohesive element with a bilinear traction-separation relationship in

Preprints (www.preprints.org) | NOT PEER-REVIEWED | Posted: 12 October 2022 doi:10.20944/preprints202210.0175.v1

ABAQUS/Standard is utilized to capture delamination. The elastic response of cohesive element is governed as

$$(3)\begin{Bmatrix} t_n \\ t_s \\ t_s \end{Bmatrix} = \begin{bmatrix} K_n & 0 & 0 \\ 0 & K_s & 0 \\ 0 & 0 & K_t \end{bmatrix} \begin{Bmatrix} \delta_n \\ \delta_s \\ \delta_s \end{Bmatrix}$$

Cohesive element occurs to damage when a quadratic stress interaction funtion involing the nominal stress ratios reaches 1. This damage criterion can be written as

$$\left(\frac{\langle \sigma_n \rangle}{N_{\max}}\right)^2 + \left(\frac{\langle \sigma_t \rangle}{T_{\max}}\right)^2 + \left(\frac{\langle \sigma_s \rangle}{S_{\max}}\right)^2 = 1 \tag{4}$$

where $\sigma_i (i = n, s, t)$ are the normal and in-plane stresses and $N_{\max}, T_{\max}, S_{\max}$ are the corresponding maximun stresss in three directions.

The mix-mode fracture energy release rate criterion of B-K[22] is particularly useful to describe the damage evolution of cohesive element, as following

$$G_{TC} = G_{IC} + (G_{IIC} - G_{IC})\left(\frac{G_{IIC} + G_{IIIC}}{G_{IC} + G_{IIC} + G_{IIIC}}\right)^{\eta} \tag{5}$$

where G_{IC} , G_{IIC} and G_{IIIC} are the critical fracture energy release rate in the normal, first and second shear directions, respectively. While η is a cohesive element parameter and is set to 1.45.

3.2.2 FEM model

The DCB tests are simulated by using ABAQUS/Standard, according to the specimen's geometry and experiment conditions, as shwon in Fig. 8. Two kinds of element types are used in this DCB model. The composite laminate is modeled with 26,000 three-dimensional eight-node linear brick elements (C3D8). In order to simulate the delamination, 2,600 linear cohesive elements are applied in the interlamiar material.

The material properties used in this model are shown in

Table 3. Especially, the critical energy release rates used to simulate cohesive element damage initiation and propagation of interlaminar material are set from experimental average value.

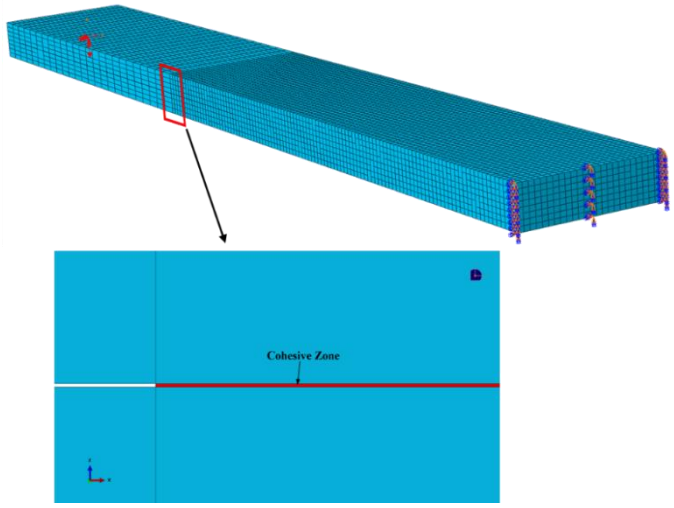

Fig. 8 The specimen's geometry and experiment conditions

Preprints (www.preprints.org) | NOT PEER-REVIEWED | Posted: 12 October 2022 doi:10.20944/preprints202210.0175.v1

Table 3 The material properties

Materials	Parameters	Values
Composite	Young's modulus	$E_{11}=E_{22}=E_{33}=20GPa$ $G_{12}=G_{13}=G_{23}=3.3GPa$
	Possion's ratio	$\nu_{12}=\nu_{13}=\nu_{23}=0.32$
Cohesive	Modulus	$E_{nn}=E_{ss}=E_{tt}=1.2\times10^{6}\,N/mm$
	Strength	$\sigma_n=50MPa,\sigma_s=\sigma_t=100MPa$
	Fracture Energy	(Original) $G_{IC}=1200\,J/m^2, G_{IIC}=G_{IIIC}=1600\,J/m^2$ (MWCNT) $G_{IC}=2300\,J/m^2, G_{IIC}=G_{IIIC}=3000\,J/m^2$

The finite element simulation results of the original and the MWCNTs toughening specimen are shown in Fig. 9. It can be seen that the deformation contour of the both are similar, but the difference is that the deformation of the MWCNTs toughening specimen is larger, which is consistent with the experimental results.

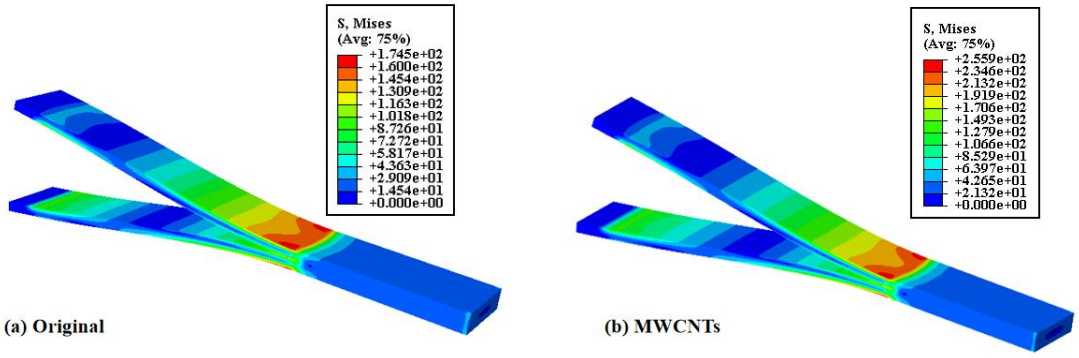

Fig. 9 The deformation contour of the Original and MWCNTs toughening specimen

The Fig. 10 shows the peel stress distribution and interlaminar damage with load displacement increase for original specimen. As can be seen from the SDEG state of Cohesive layer, the interlayer cracks expand from the middle first and then extend to both ends in a V-like expansion pattern.

Preprints (www.preprints.org) | NOT PEER-REVIEWED | Posted: 12 October 2022 doi:10.20944/preprints202210.0175.v1

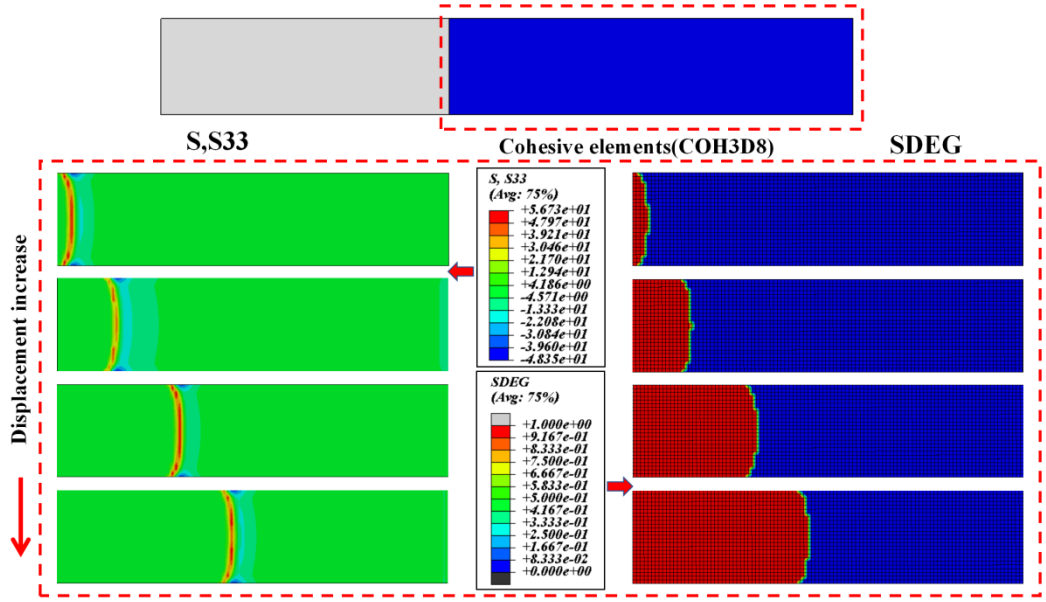

Fig. 10 Peel stress distribution and interlaminar damage with load displacement increasing for Original specimen

In

Table 3, the young's modulus E_{11} of the composite is experimentally measured. By finite element simulation, the average G_{IC} value of the Original specimens is obtained as 1200 J/m^2, and the MWCNTs toughening ones is obtained as 2300 J/m^2, which is not much different from the experimental data processing value in Section 3.1, the original group matched fairly well and the error of MWCNTs group was less than 6%.

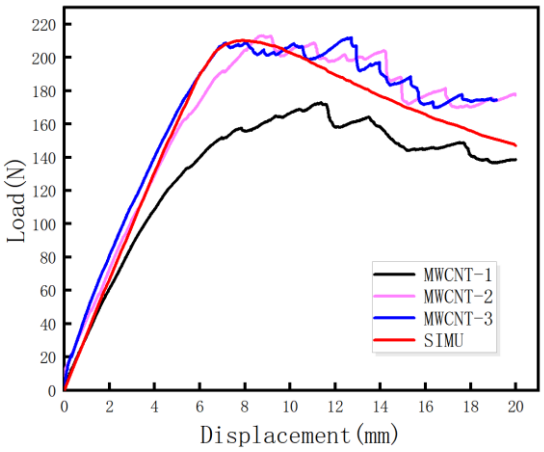

Fig. 11 is the load-displacement comparison between experiment and simulation of Original and MWCNTs specimens, it can be seen that the experimental load-displacement curve is in good agreement with the simulation curve, which indicates that the simulation results are reliable.

Preprints (www.preprints.org) | NOT PEER-REVIEWED | Posted: 12 October 2022 doi:10.20944/preprints202210.0175.v1

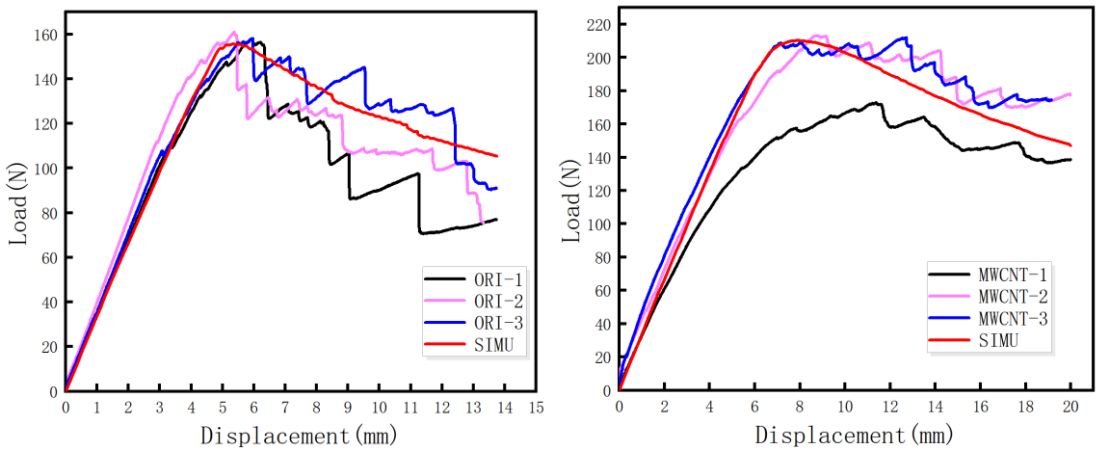

Fig. 11 The load-displacement comparison between experiment and simulation of Original and MWCNTs toughening specimens

3.3 Analysis on fracture appearance

According to the results of experimental and simulated load-displacement and G_{IC} value, the interlaminar toughening strategy by the heat repairing instrument with MWCNTs put forward by this paper is successful and significantly effective in the condition of field repair. However, only mechanical properties are obtained from the experimental data, and the toughening mechanism is still unknown. In order to reveal the interlaminar toughening mechanism, the analysis on fracture appearance is needed. Hence, fracture appearance analysis is conducted on three levels of macro-scale fracture appearance photographed by optical microscope, and meso-scale, micro-scale fracture appearance by SEM.

3.3.1 Macro-scale analysis

Fig. 12 is the photos of macro-scale fracture appearance for Original and MWCNTs toughening specimen by using optical microscope. The fracture surface of Original (Fig. 12(a)) appears smooth, and MWCNTs toughening one's (Fig. 12(b)) is relatively rough. It proves that spraying MWCNTs onto interlaminar of CFRPs affects the fracture appearance characteristic.

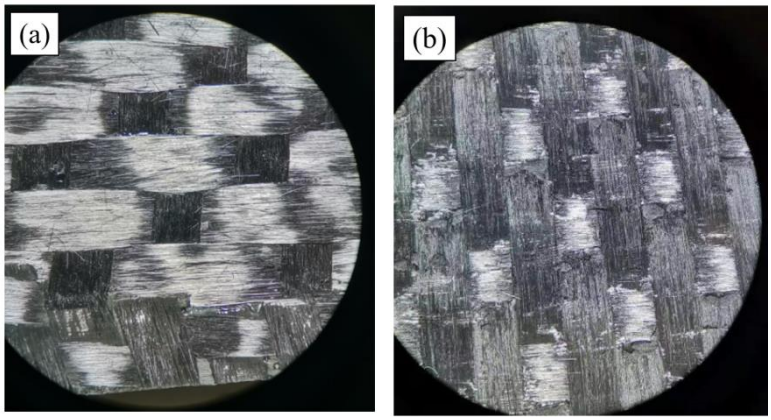

Fig. 12 photos by optical microscope: (a) Original;(b) MWCNTs toughening

3.3.2 Micro-scale analysis

Fig. 13 is the fracture appearance of original specimen photoed by SEM. With regard to the original specimens: Fig. 13(a) is the meso-scale fracture appearance of the

Preprints (www.preprints.org) | NOT PEER-REVIEWED | Posted: 12 October 2022 doi:10.20944/preprints202210.0175.v1

fiber bundle on the composite woven belts magnified 200 times. It can be obeserved that warp bundle is vertical with weft one, and the cross corners are filled with resin. The surfaces of the fiber bundles and the resin are smooth and without fiber bridging phenomenon. Fig. 13(b) and Fig. 13(c) are the micro fracture appearances of the fiber bundle magnified 1500 and 5000 times. Fiber-matrix (F-M) interface debonding and matrix cracking are clearly visible. F-M debonding surfaces are clean and smooth which indicates that interface is relatively weak and debonding happens ahead of matrix cracking. According to the SEM photos, fiber bundle breakage, matrix cracking and interface debonding of F-M can be easily obeserved, wherein the matrix cracking and the F-M interface debonding are the major modes of fracture.

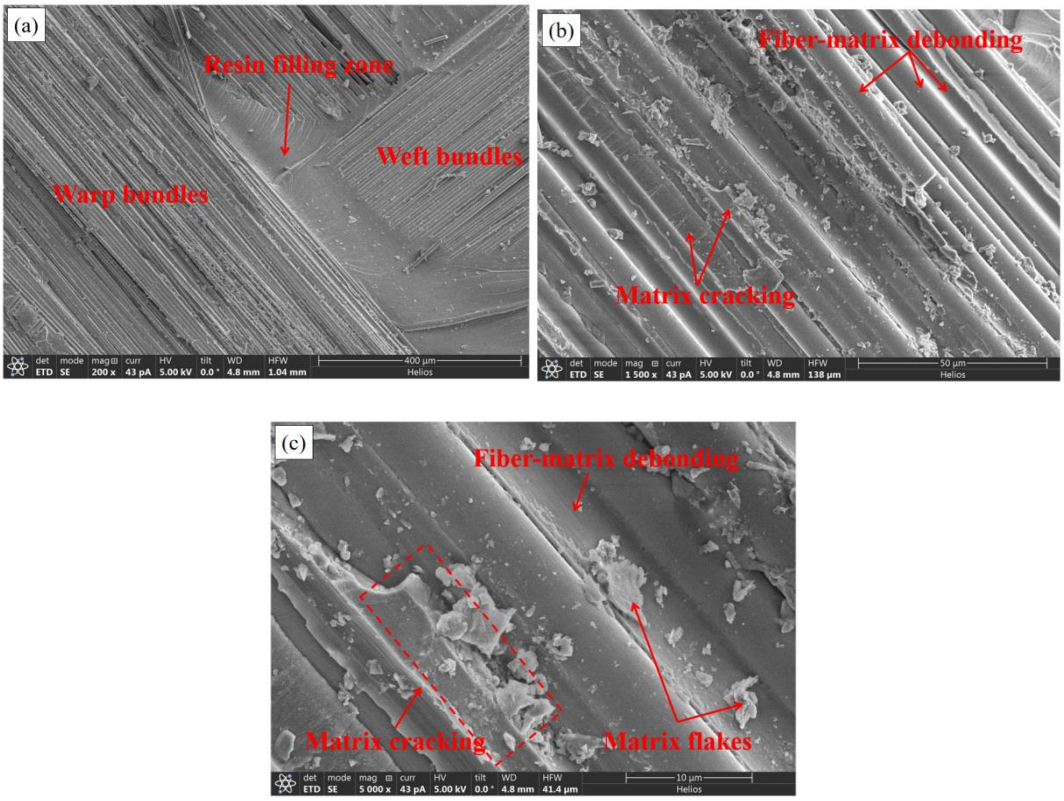

Fig. 13 SEM photos of Original specimen: a)200x; b)1500x; c)5000x

Fig. 14 shows meso-scale and micro-scale SEM photos of fracture appearance of MWCNTs toughening specimen. Fig. 14(a) is the meso-view of the bundle of composite woven belts by SEM magnified 200 times. Fig. 14(b) to Fig. 14(e) are the fiber bundle's micro fracture appearances magnified 1500 and 5000 times. Fig. 14(f) is MWCNTs pull-out picture magnified 100000 times by SEM. With regard to MWCNTs toughening specimen: (a) Fiber bundle surfaces are rough and without obvious fiber-bridging phenomenon. (b) A small quantities of fiber breakage and matrix peeling-off, the major modes of fracture are the large amount of F-M debonding and matrix cracking of mountain shape. (c) The extensive matrix cracking of mountain shape, in which MWCNTs are embedded, leads to the rough fracture surface. (d) The embedded MWCNTs are unbroken due to the high strength. And the fracture mode is MWCNTs pull-out of matrix with 1μm .

Preprints (www.preprints.org) | NOT PEER-REVIEWED | Posted: 12 October 2022 doi:10.20944/preprints202210.0175.v1

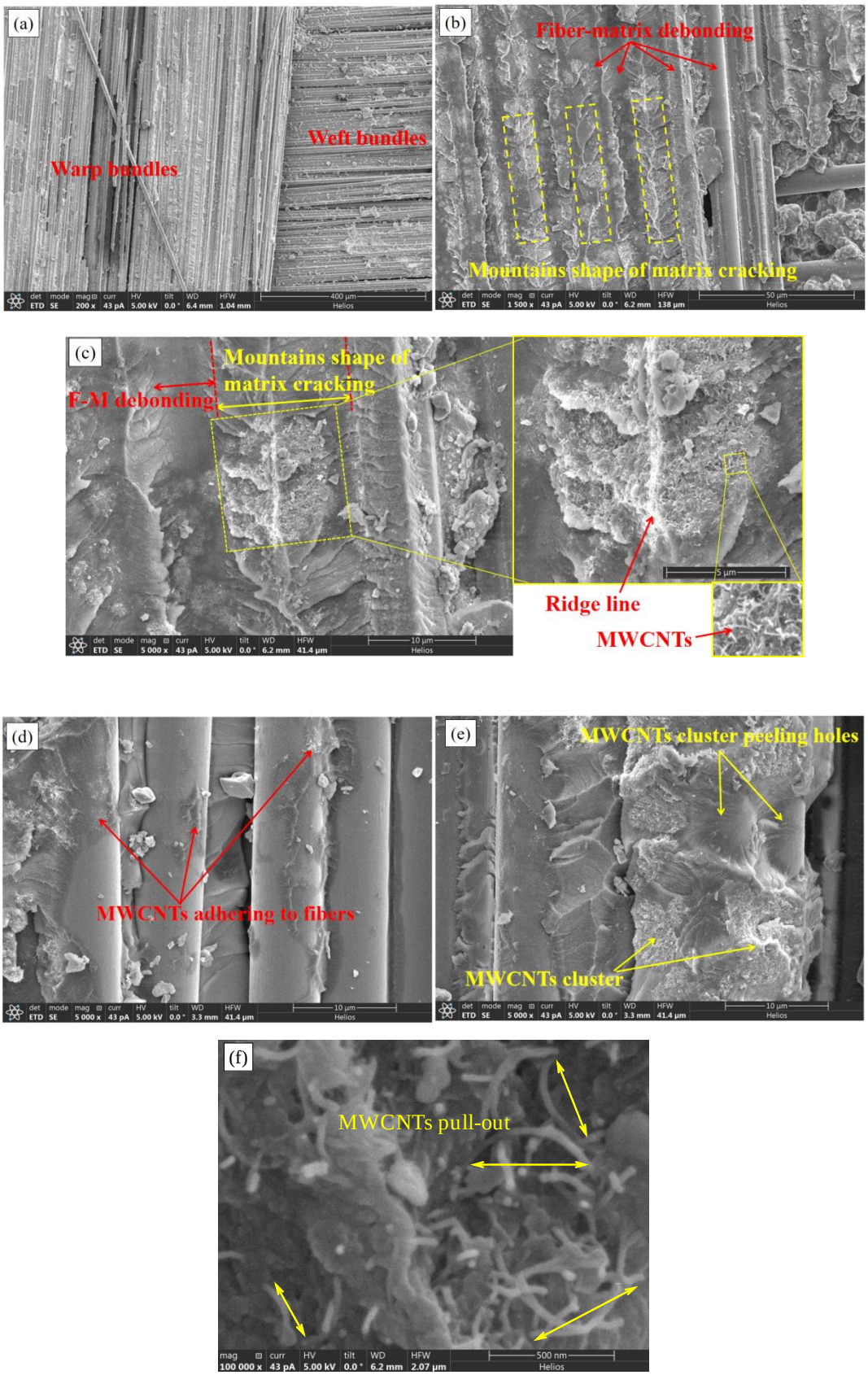

Fig. 14 Meso and micro SEM photos of fracture appearance of MWCNTs toughening specimen

3.4 Summary of toughening mechanism for MWCNTs

Preprints (www.preprints.org) | NOT PEER-REVIEWED | Posted: 12 October 2022 doi:10.20944/preprints202210.0175.v1

From the macro, meso and micro scale analysis of the fracture appearance, the precrack propagates along the preconceived interlaminar surface. On account of warp and weft bundles binding to each other, there is little fiber bridging and cracks deflect to the pure matrix of the relatively low strength, which provide a great enhancement on the interlaminar toughness with small dispersibility. Consequently, the typical interlaminar toughening mechanism of MWCNTs can be given in Fig. 15. As shown in Fig. 15(a), when the crack of model I receives tensile stress, the damage sequence of the original specimens without MWCNTs happens as follow. F-M interface debonding occurs firstly, then the debonding grows into the adjacent matrix and processes to be the new cracks which will have smooth appearences and are vertical to the tensile stress direction, and finally the F-M interface debonding cracks connect to each other till the interlaminar separates completely. However, with regard to the MWCNTs toughening ones, the cracks of F-M interface debonding grow into the matrix, then deflect wihle meeting MWCNTs, and finally give rise to the fracture appearance of mountain shape, as shown in Fig. 15(b). From the perspective of crack length, adding MWCNTs increases the crack length and enlarges the fracture surface area, which leads to an increasement of G_{IC}. On the other hand, the MWCNTs pull-out results in that the fracture toughness improving remarkably, which is the secondary major mechanism of interlaminar toughening.

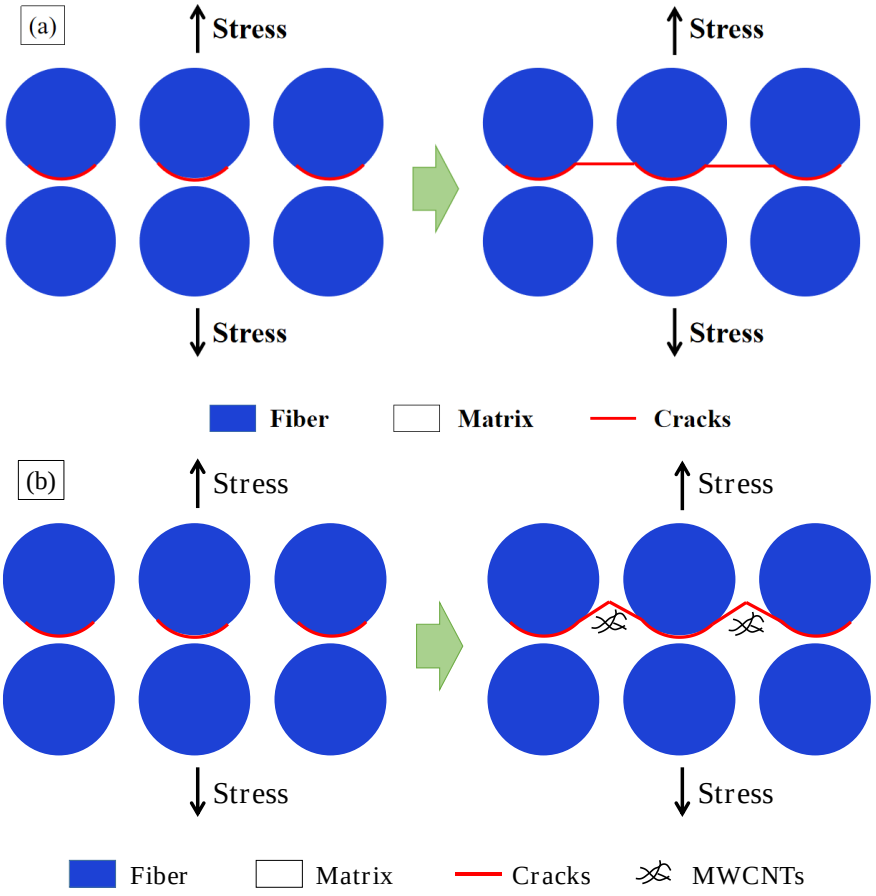

Fig. 15 The schematic of fracture mechanism: (a) Original specimens; (b) MWCNTs toughening ones

 doi:10.20944/preprints202210.0175.v1

4. Conclusion

This paper adopts experimental and simulation approach to study the improvement effect and toughening mechanism of MWCNTs on Mode I interlaminar toughness of CFRPs by heat repairing instrument in the field repair technology of the composite material. The following conclusions can be drawn:

(1) This paper proposes a convenient, low-cost and efficient field repair approach for enhancing the interlaminar fracture toughness of CFRPs. For Mode I fracture toughness, MWCNTs can greatly enhance its interlamilar toughness compared with PWCs. The average value of G_{IC} increases by 102.92%. In spite of removing the maximum G_{IC} value in MWCNTs group, it remains 95% improvement. The density of MWCNTs is 1.58 g/m^2.

(2) The load-displacement curves of the Original and MWCNTs toughening groups behave as three stages of linear increasing, nonlinear increasing and nonlinear decreasing. Comparing with the original group, not only the maximum load peak of MWCNTs toughening group increases by 19.5%, but also the slope rate of nonlinear decreasing phase decreases by 63.8%. Both of them can state that the toughening improvement of adding MWCNTs at each interface between prepreg layers is obvious.

(3) By comparing the simulation with the experiment, the good agreement of load-displacement and G_{IC} value testify that the FEM model and the mechanical parameters are validate. The bulit-in cohesive element with a bilinear traction-separation relationship is utilized to capture delamination, and the mix-mode criterion of B-K is to describe the damage evolution of cohesive element, which are suitable for the original epoxy resin and MWCNTs interlaminar simulation.

(4) The fracture appearances of original group are smooth and without obvious fiber bridging, but the surfaces of the MWCNTs group are rough. Large amount of F-M interface debonding and matrix cracking of mountain shape are the major modes of fracture accompanied with few fiber breakage and matrix peeling off. The reason for the rough surface lies in the embedded MWCNTs. The initiated cracks of F-M interface debonding deflect in the matrix while meeting MWCNTs, which leads to the fracture appearance of mountain shape. This kind of fracture appearance of mountain shape makes the crack length increase and leads to G_{IC} improvement.

Acknowledgement

The authors would like to thank the National Natural Science Foundation of China under Contracts (No. 51902256, 12172141) for the support in this research.

The authors thank Aeronautical Science Foundation of China under Contracts(No. 2020Z057053002).

The authors thank Foundation of State Key Laboratory of Structural Analysis for Industrial Equipment(No. GZ21115)

Reference

[1] B. Liu, Q. Han, X.P. Zhong, Z.X. Lu. The impact damage and residual load capacity of composite stepped bonding repairs and joints. Composites Part B: Engineering, 2019, 158: 339-351.

 doi:10.20944/preprints202210.0175.v1

[2] Pai Y, Pai K D, Kini M V. A review on low velocity impact study of hybrid polymer composites. Materials Today: Proceedings, 2021, 46: 9073-9078.

[3] Mcilhagger A T, Quinn J P, McIlhagger R. The tailoring of composite mechanical properties by textile reinforcement design. Proceeedings of the SheMet University of Ulster, 2003.

[4] Fishpool D T, Rezai A, Baker D, et al. Interlaminar toughness characterisation of 3D woven carbon fibre composites. Plastics, rubber and composites, 2013, 42(3): 108-114.

[5] Dransfield K, Baillie C, Mai Y W. Improving the delamination resistance of CFRP by stitcching—a review. Composites Science & Technology, 1994, 50(3): 305-317.

[6] Mouritz A P. Review of z-pinned composite laminates. Composites Part A: Applied Science and Manufacturing, 2007, 38(12): 2383-2397.

[7] Kobayashi S, Sugimoto K I, Nakai A, et al. Improvement in damage tolerance of CFRP laminate using the hybridization method. Composite Interfaces, 2005, 12(7): 629-635.

[8] Kim, Kyo J. Methods for improving impact damage resistance of CFRPs. Key Engineering Materials, Trans Tech Publications Ltd, 1998, 141: 149-16.

[9] Iijima S, Helical microtubules of graphitic carbon, nature, 1991, 354(6348): 56-58.

[10] Hamer S , Leibovich H , Green A. et al. Mode I and Mode II fracture energy of MWCNT reinforced nanofibrilmats interleaved carbon/epoxy laminates. Composites Science and Technology, 2014, 90: 48-56.

[11] Joshi S C, Dikshit V. Enhancing interlaminar fracture characteristics of woven CFRP prepreg composites through CNT dispersion. Journal of Composite Materials, 2012, 46(6): 665-675.

[12] Tong L, Sun X, Ping T. On the of long carbon nanotubes on Mode I delamination toughness of laminated composites. Journal of composite materials, 2008, 42(1): 5-23.

[13] Khan SU, Kim J K. Interlaminar shear properties of CFRP composites with CNF-bucky paper interleaves. The 18th International Conference on Composite Materials. 2011.

[14] Almuhammadi K, Alfano M, Yang Y. et al. Analysis of interlaminar fracture toughness and damage mechanisms in composite laminates reinforced with sprayed multi-walled carbon nanotubes. Materials & Design, 2014, 53: 921-927.

[15] B. Liu. et al. Thermosetting CFRP interlaminar toughening with multi-layers graphene and MWCNTs under Mode I fracture. Composites Science and Technology, 2019, 183: 107829.

[16] Karuppannan D. et al. Composites for reinforcement of damaged metallic aircraft wings. Journal of aerospace sciences and technologies, 2013,65(1):8-13.

[17] Monsalve A. et al. Multi-walled carbon nanotube reinforced polymer as a bonded repair for Al 2024-T3 fatigue crack growth. Matéria (Rio de Janeiro), 2018, 23.

[18] Kong, Changduk, et al. Study on Strength Recovery of Impact Damaged Composite Laminate by External Patch Repair. 2010 Asia-Pacific International

 doi:10.20944/preprints202210.0175.v1

Symposium on Aerospace Technology, 2010:852-855.

[19] B. Liu. et al. Interlaminar toughening of unidirectional CFRP with multilayers graphene and MWCNTs for Mode Ⅱ fracture. Composite Structures, 2020, 236: 111888.

[20] ASTM, D5528-01, in Standard Test Method for Mode I Interlaminar Fracture Toughness of Unidirectional Fiber-Reinforced Polymer Matrix Composites. ASTM International.

[21] Sorensen L, Botsis J. et al. Bridging tractions in Mode I delamination: Measurements and simulations. Composites Science & Technology, 2008, 68(12):2350-2358.

[22] Benzeggagh M L , Kenane M. Measurement of Mixed-Mode Delamination Fracture Toughness of Unidirectional Glass/Epoxy Composites with Mixed-Mode Bending Apparatus. Composites Science and Technology, 1996, 56(4):439-449.